DESIGN OF AUTO-FOCUSING MODULES IN CELL PHONE CAMERAS

L. K. Lai[1] and T. S. Liu[1]

[1]Department of Mechanical Engineering, National Chiao Tung University,

Hsinchu 30010, Taiwan

Emails: tsliu@mail.nctu.edu.tw

Submitted: Aug. 20, 2011 ***Accepted: Nov. 3, 2011*** ***Published: Dec. 1, 2011***

Abstract- Endowed with Hall-effect sensors and voice coil motors, cell phone cameras as intelligent systems are capable to execute auto-focusing for acquiring sharp image. For the use of cell phone cameras, this study presents an innovative auto-focusing module. When coils are powered, induced magnetic fields generate N and S poles around iron cores in the actuator. Unlike voice coil motors that employ Lorentz force, the motion of the moving part in this study is arisen from a magnetic pole property - same poles repel each other while opposite poles attract each other. Using a three-dimensional finite element method, we calculate electromagnetic and mechanical characteristics including current variation of coils, displacement and velocity of the moving part, and actuation force. Simulation results show that the proposed auto-focusing module achieves rapid response and low power consumption.

Index terms*:* Auto-focusing, cell phone camera, magnetic circuit analysis, finite element method.

I. INTRODUCTION

Endowed with Hall-effect sensors and voice coil motors, cell phone cameras as intelligent systems are capable to execute auto-focusing for acquiring sharp image. For auto-focusing (AF), an auto-focusing module has to move a lens inside a compact space. The low-current requirement of auto-focusing module is essential to conserve battery sources in mobile phones. Thus, a compact auto-focusing module for AF has to meet demands for reducing both dimension and power consumption. Various AF actuators for phone cameras have been considered by many researches [1-3]. In general, there are two types of AF actuators that are used in phone cameras. One is lens-motion AF actuating mechanisms, which may be realized by using stepping motors, voice coil motors (VCMs), or piezoelectric transducers. The stepper motors are easy to control and do not need holding power after lens movement is completed. However, the mechanical structure is complex and their volume is relatively large. Using the piezoelectric materials as actuators does not need gears and the power consumption is low, but they are sensitive to temperature and control laws are complex. The VCM has features of small volume, low cost, and easy implementation. Nevertheless, springs are usually used for open-loop positioning control. Thus, holding power is inevitable. The other type of AF actuators is the lens-modification AF mechanism, which uses liquid lens and solid-state optoelectronic devices [4-6]. Lens shapes and resulting changes of liquid refractive index are crucial to implementing AF of this type. As a consequence, this type has high technical threshold, high cost, and stringent demand on packaging. The design in this paper belongs to the first type; i.e. lens-motion AF actuating mechanisms.

The objective of the present auto-focusing module is to minimize the power consumption and the size, and above all enhancing magnetic flux density. The motion of the moving part is arisen from a magnetic field property - same poles repel each other while opposite poles attract each other, which is constantly applied to rotary motors. The mode of AF operation includes the linear motion in a given direction, short-stroke reciprocating motion. Krebs et al. [7] presented an electromagnetic actuator which involves linear or rotary movement. The device consists of permanent magnets, an iron teethed armature, and concentrated coils. An AF method [8] was presented for mobile-phone cameras to estimate the best in-focus lens position. Jin et al. [9]

presented a topology for a permanent magnet flux-switching linear machine. A prototype machine has been built to validate the theoretical analysis, and measured results agree well with those calculated by the finite element method (FEM). Chen et al. [10] presented models in finite element analysis and design of linear permanent-magnet motors with surface-mounted or interior-buried permanent magnets (PMs). Computer simulation results show that characteristics and dimensions of PMs, shapes, and armature dimensions, and all exciting currents have significant effects on motor performance. Wang et al. [11] presented analytical and measurement techniques for quantifying iron loss in short-stroke, single-phase, tubular permanent-magnet machine which is developed for direct-drive linear compressors in refrigeration applications. An optical image stabilizer system [12] that contains VCM actuators was proposed.

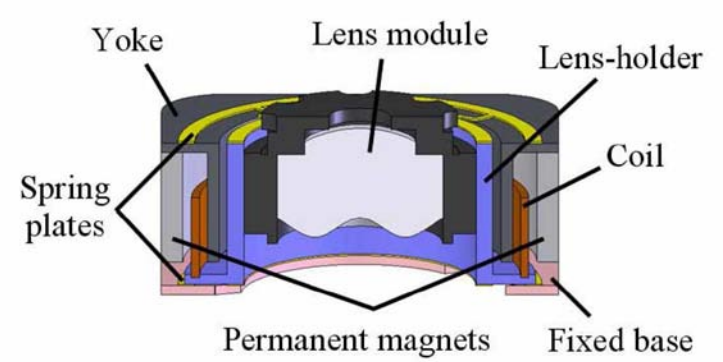

Figure 1. Structure of conventional VCM actuator [2].

II. COMPARISON OF PROPOSED AUTO-FOCUSING MODULE AND CONVENTIONAL VCM ACTUATOR

Figure 1 shows the structure of a conventional VCM actuator for AF operation in phone cameras. In general, a VCM actuator consists of two parts: a fixed part includes two PMs, a yoke, and a base; additionally, a moving part consists of a lens module, a lens holder, and a coil. Both fixed and moving parts of the VCM actuator are connected by two spring plates (one upper and one lower), which provide restoring forces to balance the Lorentz force applied to the moving part when current passes through coils. During AF actuation, the Lorentz force is larger than the sum of the moving part weight and the restoring spring force. Moreover, the spring resistance is in direct proportion to the vertical displacement of the moving part [2]. As a result, such VCM actuators typically have dimensions in the order of 10mm $\times$ 10mm $\times$ 4.6mm [13].

Unlike previous research on VCM focusing actuators, a novel auto-focusing module for AF of phone cameras is presented in this study as depicted in Figure 2. The proposed auto-focusing module structure can be divided into two parts: a moving part and a fixed part. The moving part shown in Figure 2(a) comprises a lens module with 6mm lens diameter, a lens-holder, four small PMs. The fixed part shown in Figure 2(b) comprises a Hall-effect sensor, a printed circuit board (PCB), four coils, two iron cores, and two vertical guide rods attached to a fixed base. The Hall-effect sensor is used to measure lens displacement. The overall dimensions of the auto-focusing module are as follows: length: 8.5 mm; width: 8.5 mm; height: 5 mm. When coils are powered, induced magnetic fields generate N and S poles around iron cores in the actuator. The motion of the moving part is arisen from a magnetic field property - same poles repel each other while opposite poles attract each other. The magnitude of magnetic fields is detected by a Hall-effect sensor and is converted into an output voltage signal of equivalent intensity. Comparing two actuators presented in Figures 1 and 2, it can be noted that the proposed actuator does not contain springs that are usually used in conventional VCM actuators. As a result, the device size is reduced.

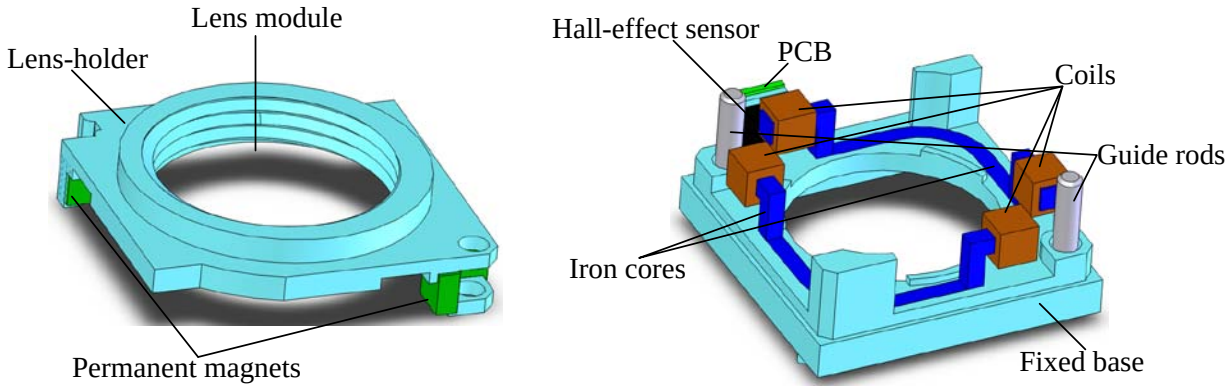

Figure 2. Components of the proposed novel auto-focusing module: (a) a moving part; (b) a fixed part.

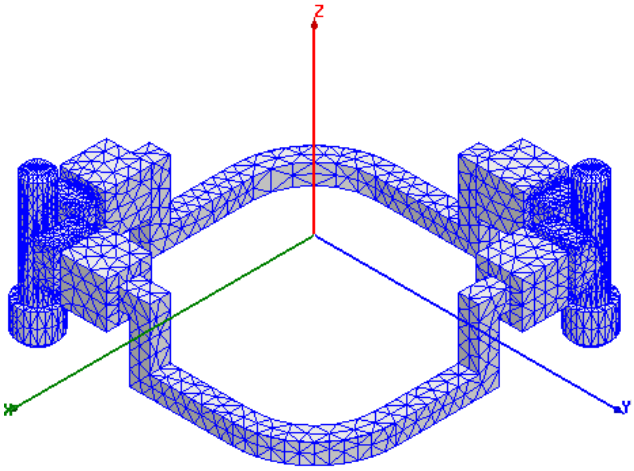

Figure 3. Finite element mesh of the auto-focusing module magnetic circuit

III. DYNAMICS MODELING

a. Electric circuit equation

To analyze the performance of auto-focusing module dynamic model, the electric circuit equation should be coupled with magnetic field equation. When the source voltage is applied to an excitation coil, the electric circuit equation is given as:

$$V = R \cdot i + L \cdot \frac{di}{dt} + \frac{d\psi}{dt} \quad , \qquad (1)$$

where V denotes the applied voltage, R is the resistance of the coil, i is the current in the coil, L is inductance of coil, and ψ is the magnetic flux linkages of the coil.

b. Magnetic field equation

The current density can be calculated by excitation currents and equivalent magnetic currents which are fundamental sources to drive the moving part in auto-focusing module. Electromagnetic field equation for auto-focusing module is formulated as

$$\nabla \times \left(\frac{1}{u} \nabla \times \vec{A} \right) + \frac{\partial \vec{A}}{\partial t} + \sigma \nabla V = \vec{J} + \nabla \times \vec{H_c} \, , \qquad (2)$$

where u is permeability of material, $\vec{A}$ is magnetic vector potential, σ is conductivity, V is scalar potential, $\vec{J}$ is input current density, $\overrightarrow{H_c}$ is coercivity of the permanent magnet.

b. Mechanical equation of motion

Important parameter of the auto-focusing module calculated from above magnetic field equation is the magnetic energy used to operate the moving part. This F_{mod} is written as below:

$$m\frac{d^2x}{dt^2}+\beta\frac{dx}{dt}=F_{\text{mod}}-F_{load}\,, \qquad (3)$$

where m denotes the moving part mass, x is the moving part displacement, β is the damping coefficient, F_{mod} is the motive force, and F_{load} is the gravity of moving part.

IV. ELECTROMAGNETIC STRUCTURE DESIGN AND SIMULATION RESULTS

a. Design of auto-focusing module structure

Having established a basic design structure for auto-focusing module, as depicted in Figure 2, design parameters including dimensions of PMs, iron cores, coils, etc. were varied to determine the best design by using FEM. Table 1 shows major parameters of the proposed auto-focusing module. When a coil is powered, a magnetic field is generated around its iron core. Accordingly, in the presence of coil currents, magnetic flux can be generated within magnetic circuits of auto-focusing module. Figures 4(a) and 4(b) show calculated distributions of magnetic flux induced within auto-focusing module under opposite-direction currents in coils, respectively. To achieve lens focusing during taking pictures, the moving part that carries optical lens has to be able to undergo opposite direction motions. It is thus essential that opposite direction coil currents result in opposite direction movements of the moving part. Since in magnetic fields repulsive forces generate between same poles while attractive forces generate between opposite poles, the permanent magnet N pole on the left-hand side in Figure 4(c) is pushed away from the iron core on the right-hand side, while the permanent magnet S pole is drawn toward the right iron core. This results in upward motion of the permanent magnet shown in Figure 4(c). On the contrary, when the coil current direction is reversed, the permanent magnet goes downward as shown in

Figure 4(d). In sum, F_{mod} acting on the movable part of auto-focusing module is aligned in the vertical direction and prompts linear motion of the moving part.

Table 1: Parameters using in auto-focusing module simulation.

Variable	**Parameter appellation and value**
Iron core material	Wrought iron
Permanent magnet material	Nd-Fe-B N48H
Length of permanent magnet	1.2 mm
Height of permanent magnet	1 mm
Thickness of permanent magnet	0.5 mm
Length of coil	1.15 mm
Height of coil	1.12 mm
Thickness of coil	0.4 mm
Winding of coil	310 turns
Air gap width	0.1 mm

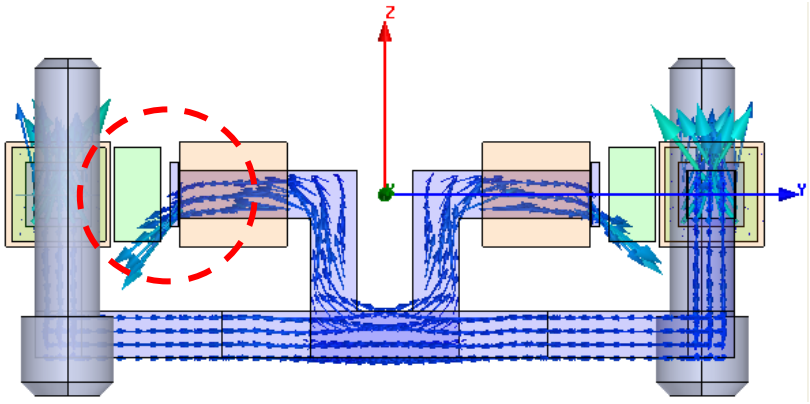

(a)

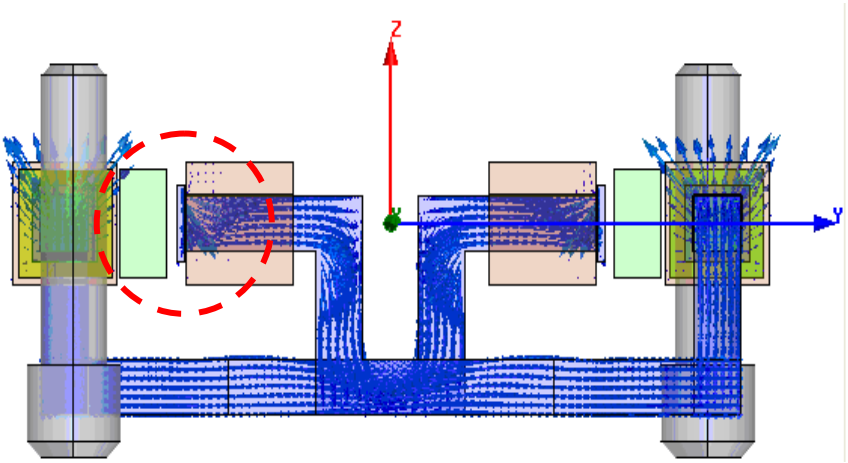

(b)

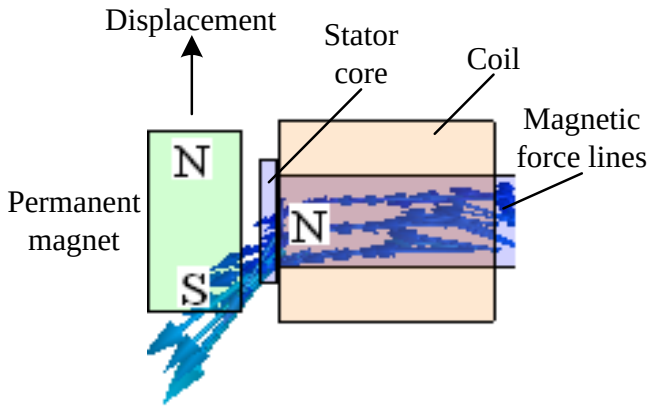

(c)

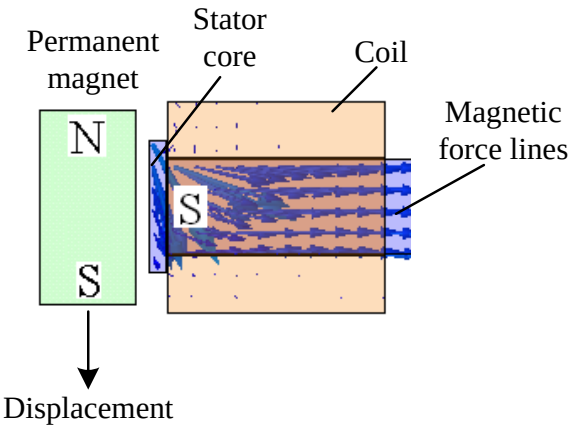

(d)

Figures 4. (a) and (b) Calculated distributions of magnetic flux under opposite-direction currents in coils. (c) Magnified view of red dashed line region in Figure 4(a). (d) Magnified view of red

dashed line region in Figure 4(b).

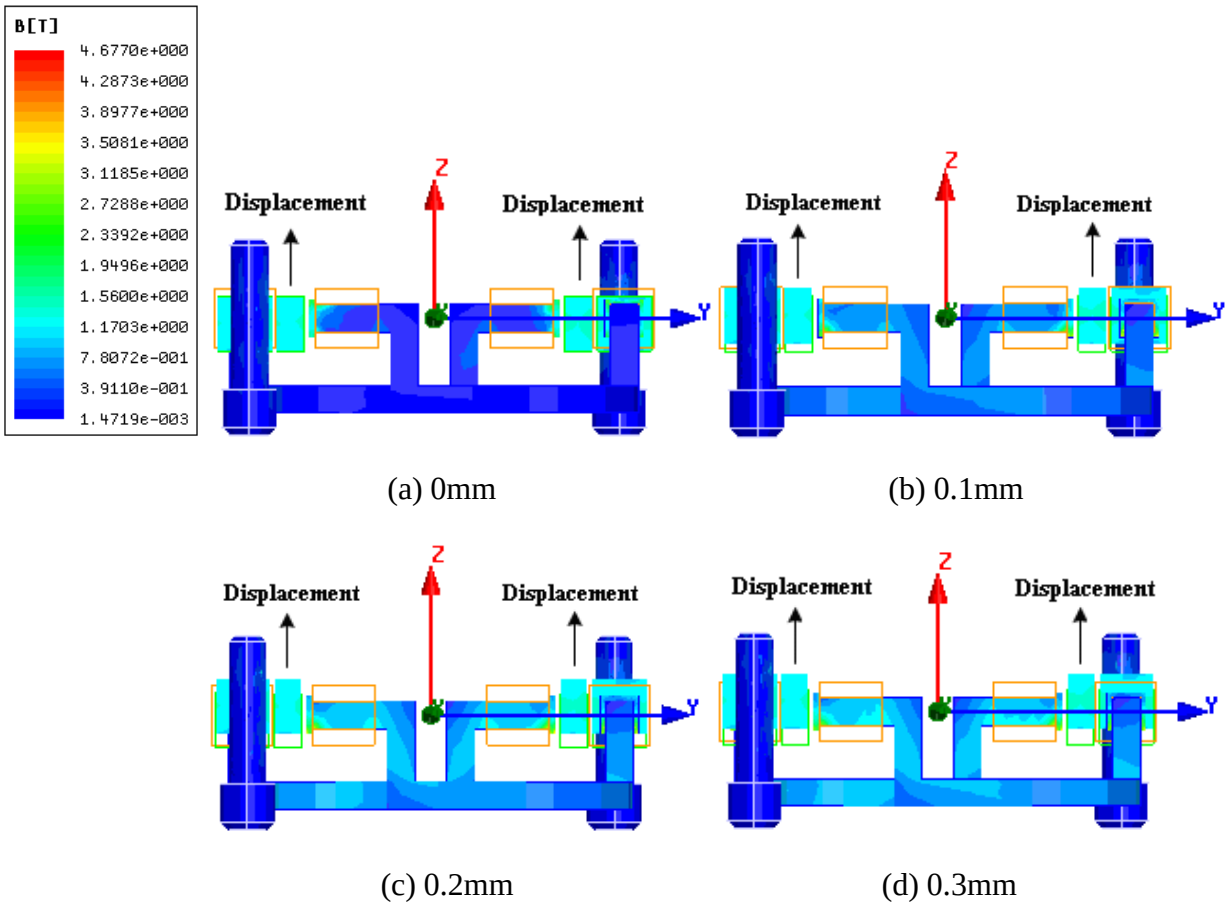

Figure 5. Magnetic flux density distribution subject to step input current and when magnet displacements reach 0, 0.1, 0.2, and 0.3mm, respectively in a, b, c, d.

Table 2. Electric parameters of coil.

Variable	Proposed auto-focusing module
Voltage	3.3 V
Resistance	47 Ω
Turns	310 turns

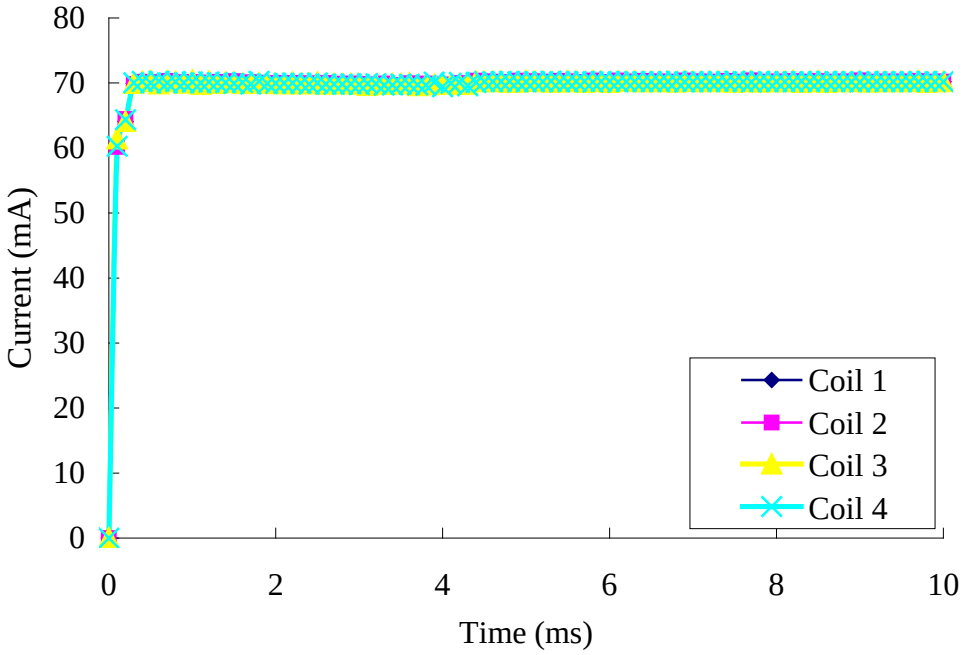

Figure 6. Current response of step input command in four coils of Figure 2(b).

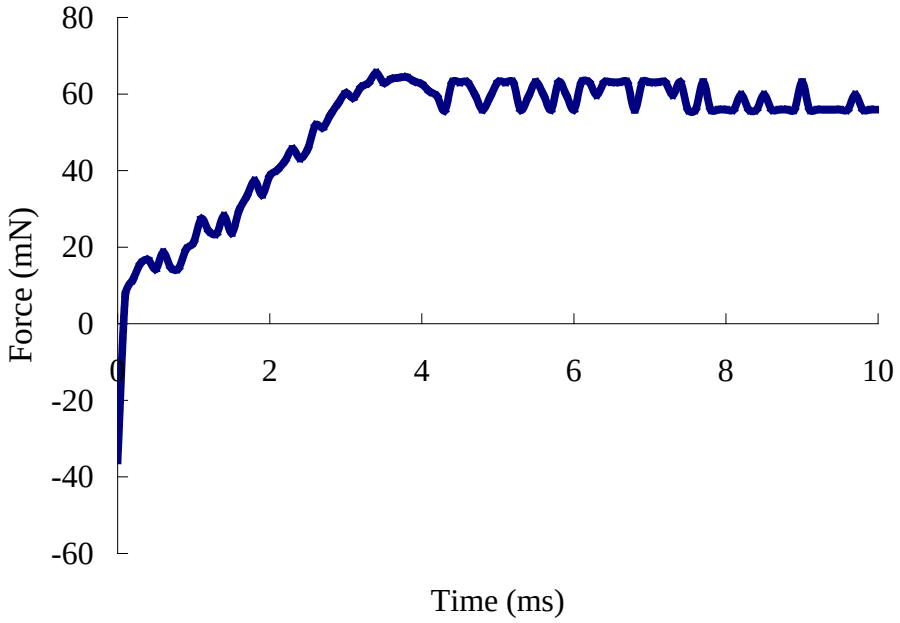

Figure 7. Generated motive force F_{mod} versus time.

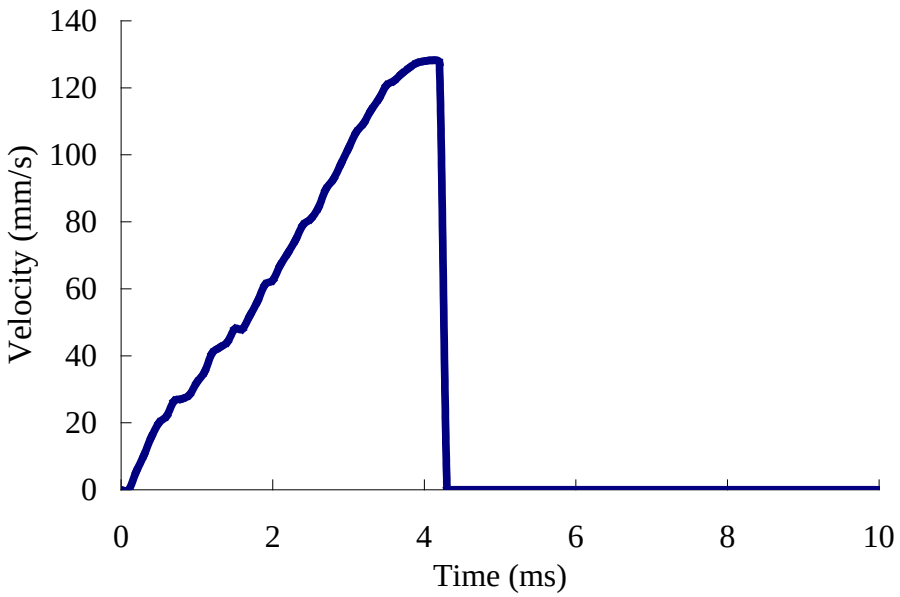

Figure 8. Simulation result for velocity versus time of moving part.

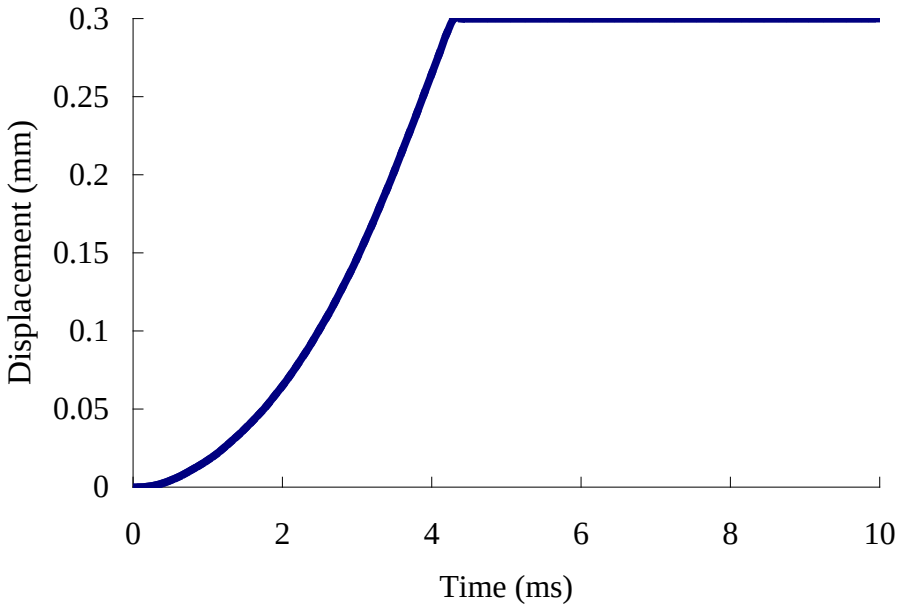

Figure 9. Displacement response of moving part from 0 to 0.3mm.

Table 3. Comparison of proposed auto-focusing module and conventional VCM actuator.

Variable	Proposed auto-focusing module	Conventional VCM actuator [13]
Size	8.5mm × 8.5mm × 5mm	10mm × 10mm × 4.6mm
Lens diameter	6mm	3mm
Air gap	0.1mm	0.3mm
Maximal current	70 mA	80 mA

b. Dynamic performance

Dynamic performance of auto-focusing module is analyzed by FEM. Motive force F_{mod}, displacement, and velocity in the auto-focusing module model are solved by using equations (1)-(3). In coupled analysis, we consider nonlinearity of material, external electric circuit to coil, damping and mass of the moving part to obtain accurate results of the auto-focusing module model. Figures 5(a)–(d) illustrate the upward displacement of permanent magnets in the moving part and magnetic flux density distribution with step input current in four coils depicted in Figure 2(b). As permanent magnet N pole and iron core N pole are away from each other with the order of Figures 5(a), 5(b), 5(c), 5(d), repulsive force becomes weaker while attractive force becomes stronger. When the permanent magnet S pole and iron core N pole are closer to each other, the magnetic field of the iron core becomes stronger. Since the magnetic flux density is related to the magnetic field by [17]

$$\mathbf{\Phi_m} = \iint_S \boldsymbol{B} \cdot d\boldsymbol{S}, \tag{4}$$

where $\mathbf{\Phi_m}$ is the magnetic flux, $\boldsymbol{B}$ is the magnetic field, $\boldsymbol{S}$ is the integral of the magnetic field over the area of the surface, the magnetic flux density is proportional to the magnetic field in Figures 5(a)-(d). Therefore, the magnetic flux density in Figure 5(c) is the strongest. Electric parameter values are depicted in Table 2. Figure 6 shows four curves of step input current flowing in four coils as depicted in Figure 2(b). The four curves coincide. The peak value of the current is 70 mA. This represents a current reduced by 12.5% compared to the conventional actuator, and leads to a significant improvement in the power efficiency of the device. Table 3 compares principal characteristics between the proposed auto-focusing module and a conventional VCM [13]. Figure

7 shows variation of the motive force F_{mod} acting on the moving part. If F_{mod} is greater than the weight of the moving part, the moving part moves up. Figure 8 shows velocity of the auto-focusing module. As depicted in Figure 4(d) where auto-focusing module displaces 0.3mm and reaches the upper limit of the stroke. Figure 9 shows displacement of the auto-focusing module at 0.3 mm. At 0.2 ms, the auto-focusing module begins to move and operation is completed at 4.3 ms. Since the movement time is less than 10 ms, as far as response time is concerned the proposed auto-focusing module satisfies requirements in the market standard [2]. Compared with the conventional VCM actuator, the proposed auto-focusing module has a smaller physical size, larger F_{mod} due to smaller current of 70mA acting on the larger lens of 6mm, less magnetic flux leakage, and smaller current of 70 mA at 3.3V. As a consequence, the proposed auto-focusing module outperforms the conventional VCM.

V. CONCLUSION

This study has presented a novel compact auto-focusing module for AF of phone cameras. The proposed auto-focusing module can be applied to phone cameras having over eight megapixels with a diameter 6mm of lens size. Moreover, unlike conventional voice coil motors that employ Lorentz force, the motion of the moving part is arisen from a magnetic field property - same poles repel each other while opposite poles attract each other. Using a three-dimensional finite element method, we calculate electromagnetic and mechanical characteristics such as current variation of coils, displacement of the moving part, velocity, and F_{mod} of the auto-focusing module. When compared to conventional VCM actuators in simulation results, the proposed auto-focusing module has smaller physical size, larger F_{mod}, less magnetic flux leakage, and smaller current. The most important thing is that the response time of the novel auto-focusing module is 4.3 ms less than the usual 10 ms. The result of response time satisfy the response requirements in the market standard [2]. As a result, the proposed novel auto-focusing module represents a creative and promising design for AF applications in mobile phone cameras. Furthermore, it can also be used in consumer electronic devices such as speakers, optical disk drives, hard disk drives, camera, etc.

ACKNOWLEDGEMENT

This work was supported by National Science Council in Taiwan, ROC under Grant No. NSC99-2221-E009-020-MY2.

REFERENCES

[1] M. J. Chung and S. Y. Son, “Development of compact auto focus actuator for camera phone by applying new electromagnetic configuration,” J. Mech. Sci. Technol. (KSME Int. J.) 20, pp. 2087-2093, 2006.

[2] C. S. Liu and P. D. Lin, Po-H. Lin, S. S. Ke, Y. H. Chang, and Ji-B. Horng, “Design and characterization of miniature auto-focusing voice coil motor actuator for cell phone camera applications, ” *IEEE Trans. Magn.*, vol. 45, no. 1, pp. 155-159, Jan. 2009.

[3] H. P. Ko, H. Jeong and B. Koc, “Piezoelectric actuator for mobile auto focus camera applications,” J. Electroceram. 23, pp. 530-535, 2009.

[4] S. Kuiper and B. H. W. Hendriks, “Variable-focus liquid lens for miniature cameras,” Appl. Phys. Lett. 85 , pp. 1128-1130, 2004.

[5] H. Ren and S. T. Wu, “Variable-focus liquid lens,” Opt. Express 15, pp. 5931-5936, 2007.

[6] H. K. Lee, N. J. Choi, S. Jung, K. H. Park, H. Jung, J. K. Shim, J. W. Ryu, and J. Kim, “Electroactive polymer actuator for lens-drive unit in auto-focus compact camera module,” ETRI Journal, vol.31, no.6, pp.503-511, Dec. 2009.

[7] G. Krebs, A. Tounzi, B. Pauwels, D. Willemot, and F. Piriou, “Modeling of a linear and rotary permanent magnet actuator,” *IEEE Trans. Magn.*, vol. 44, no. 10, pp. 4357-4360, Nov. 2008.

[8] J. W. Han, J. H. Kim, H. T. Lee, and S. J. Ko, “A Novel Training Based Auto-Focus for Mobile-Phone Cameras,” *IEEE Transactions on Consumer Electronics*, Vol. 57, No. 1, February 2011

[9] M. J. Jin, C. F. Wang, J. X. Shen, and B. Xia, “A modular permanent-magnet flux-switching linear machine with fault-tolerant capability,” *IEEE Trans. Magn.*, vol. 45, no. 8, pp. 3179-3185, Aug. 2009.

[10] Y. M. Chen, S. Y. Fan, and W. S. Lu, "Performance analysis of linear permanent-magnet motors with finite-element analysis," *IEEE Trans. Magn.*, vol. 44, no. 3, pp. 377-385, Mar. 2008.

[11] J. Wang, T. Ibrahim, and D. Howe, "Prediction and measurement of iron loss in a short-stroke, single-phase, tubular permanent magnet machine," *IEEE Trans. Magn.*, vol. 46, no. 6, pp. 1315-1318, June 2010.

[12] D. H. Yeom, "Optical image stabilizer for digital photographing apparatus," *IEEE Transactions on Consumer Electronics*, Vol. 55, No. 3, Aug. 2009.

[13] [Online]. Available: http://www.shicoh.com/e/index.htm.

[14] J. K. Kim, C. G. Lee, S. Y. Jung, and S. C. Hahn, "Optimal design and characteristic analysis of permanent magnet actuator using parallel genetic algorithm," *CEFC*, May 2008.

[15] S. Fang, H. Lin, and S.L. Ho, "Transient co-simulation of low voltage circuit breaker with permanent magnet actuator," *IEEE Trans. Magn*, vol. 45, no. 4, pp. 1242– 1245, March 2009.

[16] I. Yatchev and E. Ritchie, "Simulation of dynamics of a permanent magnet linear actuator," World Academy of Science, Engineering and Technology 2010.

[17] B. D. Cullity, Introduction to magnetic materials. Hoboken, N. J.: IEEE/Wiley, 2009.